

2001

## Synthesis and Characterization of Hydrus Ruthenium Oxide-Carbon Supercapacitors

Manikandan Ramani

*University of South Carolina - Columbia*

Bala S. Haran

*University of South Carolina - Columbia*

Ralph E. White

*University of South Carolina - Columbia, white@cec.sc.edu*

Branko N. Popov

*University of South Carolina - Columbia, popov@engr.sc.edu*

Follow this and additional works at: [https://scholarcommons.sc.edu/eche\\_facpub](https://scholarcommons.sc.edu/eche_facpub)



Part of the [Chemical Engineering Commons](#)

---

### Publication Info

*Journal of the Electrochemical Society*, 2001, pages A374-A380.

This Article is brought to you by the Chemical Engineering, Department of at Scholar Commons. It has been accepted for inclusion in Faculty Publications by an authorized administrator of Scholar Commons. For more information, please contact [digres@mailbox.sc.edu](mailto:digres@mailbox.sc.edu).



## Synthesis and Characterization of Hydrous Ruthenium Oxide-Carbon Supercapacitors

Manikandan Ramani,\* Bala S. Haran,\*\* Ralph E. White,\*\*\*  
and Branko N. Popov,\*\*,z

Center of Electrochemical Engineering, Department of Chemical Engineering, University of South Carolina,  
Columbia, South Carolina 29208, USA

It is shown that composite Ru oxide-carbon based supercapacitors possess superior energy and power densities as compared to bare carbon. An electroless deposition process was used to synthesize the ruthenium oxide-carbon composites. Ru is dispersed on the carbon matrix as small particles. The effect of electrochemical oxidation and temperature treatment on the material performance has been studied extensively. Increasing the oxidation temperature reduces the proton transport rate and also increases the degree of crystallinity of the deposits. This adversely affects the performance of the composite. Loading a small amount of Ru oxide (9 wt %) on carbon increases the capacitance from 98 to 190 F/g.

© 2001 The Electrochemical Society. [DOI: 10.1149/1.1357172] All rights reserved.

Manuscript submitted July 10, 2000; revised manuscript received January 8, 2001.

Electrochemical capacitors or supercapacitors are novel power devices, which lie between batteries and conventional dielectric capacitors in terms of energy and power densities. The major focus on developing supercapacitor materials has been on utilizing the double layer capacitance formed at the interface of the electrode and the electrolyte. Although this capacitance per unit area is low ( $10\text{--}30\text{ }\mu\text{F}/\text{cm}^2$ ), it can be enhanced significantly by the use of materials with high specific surface areas.<sup>1,2</sup> The value also has significant range due to the presence of edge sites and use of surface functional groups to activate the carbon.<sup>2</sup> Various carbonaceous materials with their large specific surface areas and good conductivity serve as ideal candidates for supercapacitor devices.<sup>1</sup> Recent research has also focused on the development of an alternate class of supercapacitors based on fast reversible faradaic reactions.<sup>3–12</sup> Commonly, known as “pseudocapacitors” they consist of various transition oxides, transition metal nitrides, and conducting polymers.

Of these, much progress has been achieved on the metal oxides namely  $\text{RuO}_2$ ,  $\text{Co}_3\text{O}_4$ , and  $\text{NiO}_2$ . Nickel oxide films have been synthesized both electrochemically<sup>4</sup> and also by the sol-gel process.<sup>5</sup> A specific capacitance of  $50\text{--}64\text{ F/g}$ , with specific energy and power of  $25\text{--}40\text{ kJ/kg}$  and  $4\text{--}17\text{ kW/kg}$ , respectively, has been achieved. Crystalline  $\text{RuO}_2$  with a surface area of  $120\text{ m}^2/\text{g}$  has a specific capacitance of  $350\text{ F/g}$ .<sup>6</sup> Hydrous ruthenium oxide formed by a sol-gel process yields a specific capacitance of  $760\text{ F/g}$  and a specific energy of  $27\text{ Wh/kg}$ .<sup>7,10</sup> Cobalt oxides synthesized by a similar sol-gel process also exhibit pseudocapacitive behavior. The capacitance of transition metal oxides depends on the mass of active material consumed, with bulk diffusion processes controlling this utilization.

In contrast to pseudocapacitors, the capacitance of carbon-based materials is directly linked to their specific surface area. However, increasing this area beyond a certain point does not translate to a similar increase in the capacitance. The increased surface area arises due to the formation of micropores smaller than  $10\text{ }\text{\AA}$ .<sup>1</sup> These pores remain inaccessible to the electrolyte and hence do not form a double layer. Therefore, energy and power density realizable from any carbonaceous material is not large. Alternatively, pseudocapacitors have significantly large energy densities as compared to carbon-based double layer capacitors. In addition, electrical conductivity of metal oxides ( $\text{RuO}_2$ ) is far greater than carbon and leads to higher inherent power densities or lower resistance-capacitance (RC) time constants. These advantages of pseudocapacitors are offset by their high cost as compared to carbon. The advantages accrued from

carbon-based materials could be combined with those of the transition metal oxides leading to the development of a new brand of electrochemical capacitors. Development of composite double-layer faradaic pseudocapacitors would result in utilizing both the faradaic capacitance of the metal oxide and the double layer capacitance of the carbons. Few studies have focused on developing supercapacitors utilizing both these phenomena.

The goal of this research is to develop composite carbon metal oxides using an electroless deposition technique. In this paper, we focus on the development of Ru oxide-carbon composite capacitors. Synthesizing Ru oxide-carbon composites has been achieved either by sputtering Ru on carbon and electrochemically oxidizing it<sup>11,12</sup> or by sol-gel processes.<sup>8</sup> An alternate synthesis route based on electroless deposition of Ru on carbons has been developed. Electrochemical and material characterization studies on this material are also reported.

### Experimental

Ruthenium oxide-carbon composites were synthesized by controlled deposition of Ru onto carbon and subsequent oxidation. Activated carbon (Westvaco) of surface area  $1200\text{ m}^2/\text{g}$  was chosen as the substrate. The carbon particles were immersed in an aqueous bath of  $0.014\text{ M}$  ruthenium chloride,  $0.27\text{ M}$  sodium hypophosphite,  $0.014\text{ M}$  diammonium hydrogen citrate, and  $0.07\text{ M}$  ammonium oxalate. The pH of the bath was maintained at  $\sim 9.5$  by periodic addition of NaOH. The bath temperature was kept at  $90^\circ\text{C}$ . Small particles of ruthenium were deposited on the carbon surface by autocatalytic process. Varying the time of deposition or the amount of  $\text{RuCl}_3$  used, the amount of metal loaded on carbon can be controlled. The advantage of electroless deposition over other techniques is that it can be used for synthesizing large amounts of material. In this study, the total loading was kept constant at  $9\text{ wt } \%$  of final active material. The deposition time was extended until all the Ru had been exhausted from the bath. This was inferred from changes in the electrolyte pH. During the autocatalytic process, protons ( $\text{H}^+$ ) are produced, which result in lowering the solution pH. Once the plating process ends, no more  $\text{H}^+$  ions are produced and the pH remains stable. An accurate estimate of the amount of Ru deposited was determined by potentiometric titration of a known volume of the spent electrolyte with ceric sulfate.

**Material characterization.**—After deposition, the filtrate was dried at  $50^\circ\text{C}$  for  $10\text{ h}$ . The presence of ruthenium over the substrate was confirmed by energy dispersive analysis by X-ray (EDAX). Hitachi S-2500 with iridium software was used for EDAX and scanning electron microscopy (SEM) studies. Electron probe microanalysis (EPMA) analysis was also performed on the deposit with a model SX-50 electron microprobe (Cameca Inc). The chemical composition of different components in the deposit was deter-

\* Electrochemical Society Student Member.

\*\* Electrochemical Society Active Member.

\*\*\* Electrochemical Society Fellow.

z E-mail: popov@engr.sc.edu

mined. Surface area of the composites was determined by Brunauer-Emmett-Teller (BET) analysis using Pulse Chemisorb 2000 (Micromeritics inc.) The surface area of the coated material was 1060 m<sup>2</sup>/g by BET. X-ray diffraction (XRD) was performed on the samples to determine the degree of crystallinity of the deposits. The XRD data were collected on a Rigaku D/Max-2200 powder X-ray diffractometer using Bragg-Brentano geometry with Cu K $\alpha$  radiation. Thermogravimetric analysis (TGA) was done to determine change in sample weight with increase in temperature.

**Electrochemical characterization.**—Metal-loaded carbon was mixed with 5% polytetrafluoroethylene and ground to form a paste. Pellets 130  $\mu$ m thick, 3–5 mg in weight were prepared by cold-pressing the paste between two tantalum meshes. Tantalum was used as the current collector because it is inert in acidic solutions and does not contribute to faradaic reactions. Electrochemical characterization of these materials was done using a three-electrode setup with 1 M H<sub>2</sub>SO<sub>4</sub> as the electrolyte, saturated calomel electrode (SCE) as the reference and Pt as the counter electrode. The dimensions of the counter electrode were 2.1  $\times$  2.0 cm. All measured potentials are referred to the SCE reference electrode. Cyclic voltammetry (CV) and galvanostatic charge-discharge studies were used to characterize the materials using an EG&G galvanostat/potentiostat (model 273 A).

In all cases, the potential window of operation was determined by CV studies (usually 0.9 V). The charge associated with CVs gave us an idea of the current to be used in galvanostatic charge-discharge studies.

**Oxidation studies.**—The deposited ruthenium particles were oxidized electrochemically or by heat-treatment. Electrochemical oxidation was performed by holding the potential constant at 0.75 V for 3 h. A similar approach was used by Miller *et al.*<sup>11</sup> for converting their sputtered Ru thin films to oxides. Zheng *et al.*<sup>7,10</sup> obtained hydrated Ru oxides by a sol-gel precipitation process. The precipitate was subsequently converted to a powdered form by heating to a temperature between 25 and 400°C. In our case, the effect of temperature on Ru oxide performance was studied by heating the dried samples at 100, 125, 150, 200, 300, and 400°C in an oxygen atmosphere for 3 h. XRD patterns were obtained from the different annealed samples.

## Results and Discussion

**Nature of deposits.**—Figure 1a shows the SEM image of the composite. The carbon surface is dark and the Ru deposits are seen as small white clusters. Because the total area of the carbon is enormous (1200 m<sup>2</sup>/g), it is not possible to cover the entire surface of the carbon with Ru. Figure 1b shows the TEM image of the composite material. Ru oxide particles of size 100 nm are seen dispersed on the surface of the carbon. EDAX analysis confirms the presence of Ru on the carbon surface. Figure 2 shows the EPMA imaging of the constituents in the deposit. Figure 2a shows the RuO<sub>2</sub>-carbon composite. Figure 2b shows the underlying carbon matrix. Figure 2c depicts the ruthenium phase over the surface of carbon. It can be seen from Fig. 2b and c that the ruthenium phase covers the carbon matrix in the form of small particles. Oxygen was found on the substrate along with the ruthenium phase (Fig. 2d).

**Crystalline structure.**—The structure of autocatalytically deposited Ru coatings undergoes important changes because of heat-treatment. The structure of the RuO<sub>2</sub>-carbon composite annealed at different temperatures was characterized using an X-ray diffractometer and the resulting XRD patterns are shown in Fig. 3. At low temperatures the material is amorphous in nature and this is confirmed by the broad diffuse patterns seen at 50 and 100°C. On increasing the temperature above 200°C, the peak intensities increase and the composite becomes crystalline in nature. At 400°C, the width of the peaks decreases drastically and the XRD pattern corresponds to that of anhydrous RuO<sub>2</sub>. The results show that change in temperature significantly alters the crystalline size. Zheng and Jow<sup>7</sup>

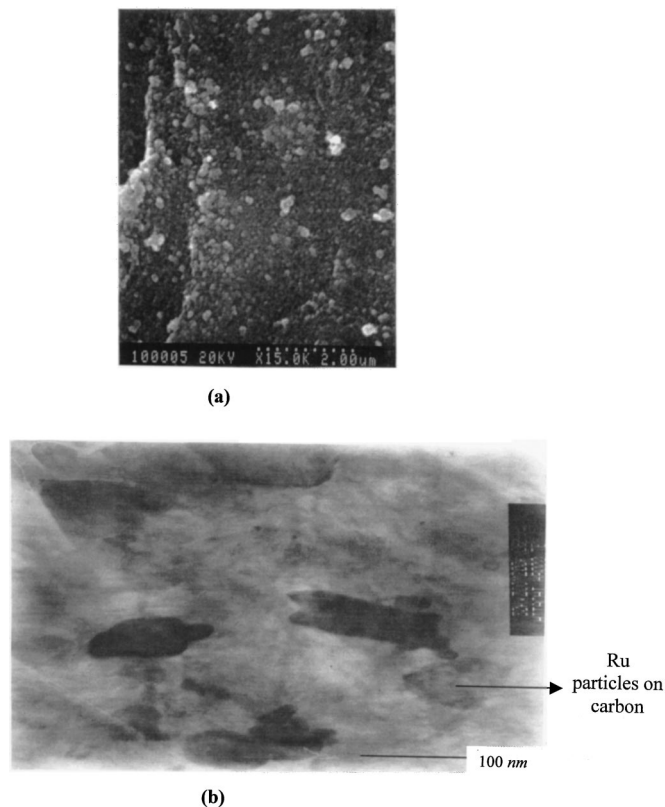


**Figure 1.** (a) SEM images of the electroless Ru deposits on carbon substrate. (b) TEM analysis of Ruthenium oxide-carbon composite.

observed that their sol-gel derived RuO<sub>2</sub>·2H<sub>2</sub>O changed from amorphous to crystalline form on heating to 400°C. The diffraction peaks obtained in this study agree with the results presented by previous researchers. A detailed analysis of the effect of heating on RuO<sub>2</sub> composition has been done by McKeown *et al.*<sup>9</sup> Crystalline RuO<sub>2</sub> has a rutile type structure. Hydrated RuO<sub>2</sub> has a disordered rutilelike structure, with structural water disrupting the three dimensional rutile structure.<sup>9</sup> Another important point observed was that at low temperatures, the time of heating does not alter the structure of the composite. RuO<sub>2</sub>-carbon composite heated at 100°C for 12 h exhibits the same structure as that heated for 3 h (shown in Fig. 3). This is a characteristic feature of electroless deposits and has been seen for Ni-P coatings where heat-treatment at 200°C for 20 h does not alter the XRD peaks, but heating at 400°C for only 1 min leads to significant changes in structure.<sup>13</sup>

Figure 4 presents the thermogravimetric analysis of the sample. The TGA analysis reveals continuous removal of water from the sample as it is heated. The percent change in weight on heating the sample from 25 to 300°C is 12%. Because decomposition of RuO<sub>2</sub> to Ru metal does not occur at temperatures less than 1000°C, McKeown *et al.*<sup>9</sup> attributed the weight loss on heating to loss of bound water. In our case, this 12% weight loss corresponds to a composition of RuO<sub>2</sub>·H<sub>2</sub>O. The final powders could also be Ru(OH)<sub>3</sub> or Ru(OH)<sub>2</sub>·H<sub>2</sub>O because their molecular weights are also the same.<sup>10</sup>

**Studies on activated carbon.**—To obtain a measure of the double layer capacitance of activated carbon, CVs were performed in the potential range of 0.0 to 0.90 V vs. SCE. Figure 5A presents the CVs of bare carbon both during anodic and cathodic sweeps at 1 mV/s. The constant current seen with variation in potential is characteristic of a capacitive behavior. Similar studies on the tantalum current collector showed that tantalum is inert in acidic conditions in our potential range of operation. The capacitive behavior in carbons



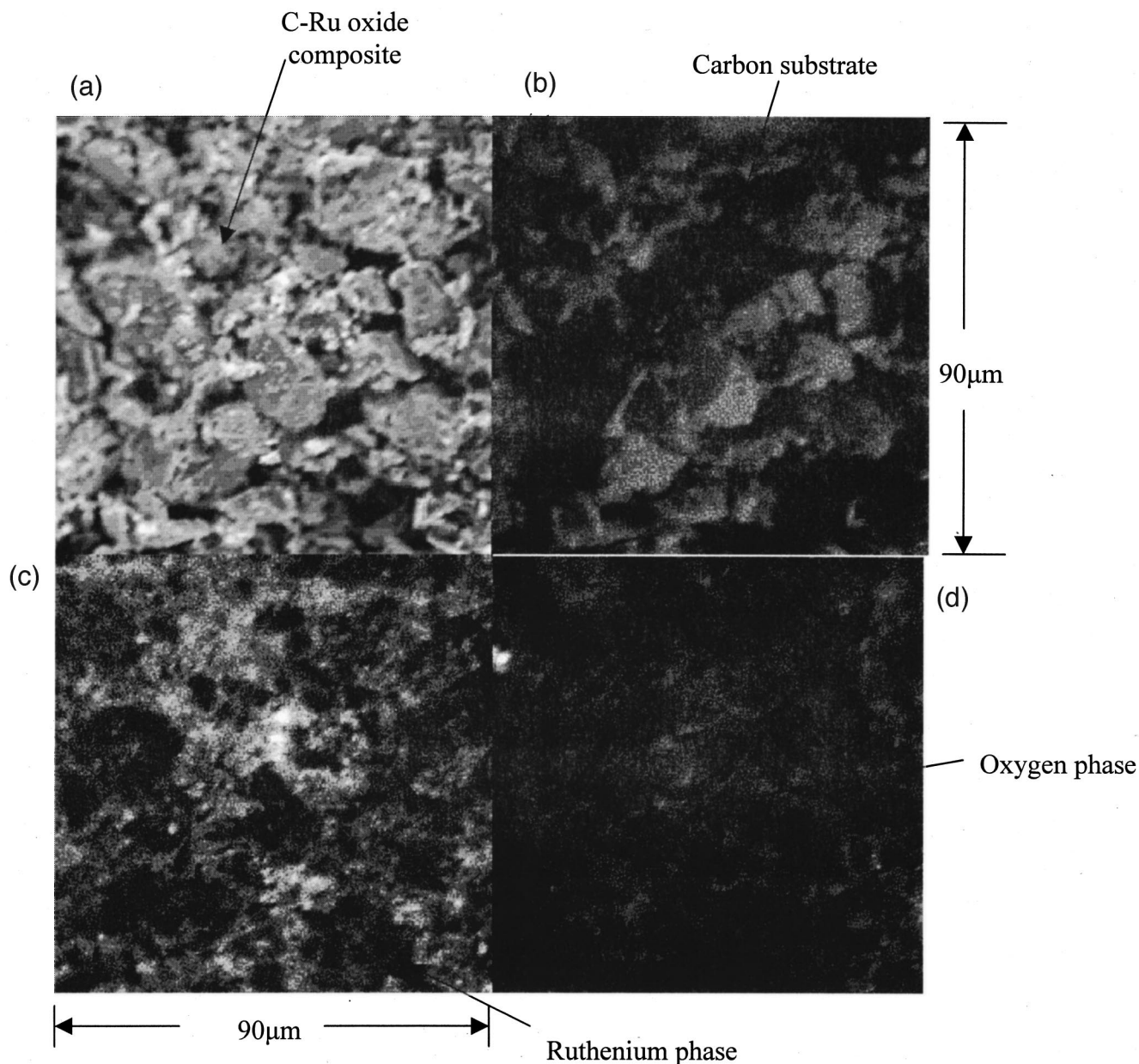


**Figure 2.** EPMA analysis on the Ru-plated carbon. (a) Discrete ruthenium particles over carbon matrix, (b) carbon matrix, (c) ruthenium phase dispersed over the matrix, (d) oxygen present in the composite.

arises due to the charging and discharging of the double layer at the carbon-electrolyte interface. The total capacitance can be calculated from Fig. 5A by

$$C = \frac{1}{w\Delta V} \int_0^1 i dt \quad [1]$$

where  $w$  is the mass of active material,  $i$  is the anodic/cathodic current flowing for time  $dt$ . The potential window  $\Delta V$  is the range in which the anodic (positive) or cathodic (negative) current flows. A net specific capacitance of 98 F/g was calculated from the CVs in Fig. 5A. In general, the double layer capacitance at an electrode surface is in the range of 10–30  $\mu\text{F}/\text{cm}^2$  as referred earlier. In conventional planar electrodes, this does not amount to much because the surface area in these cases is very small. Much research has been done on synthesizing various activated carbons, aerogels, activated carbon fibers, and cloths with large surface areas. In our case, the

activated carbon has an active surface area of 1200  $\text{m}^2/\text{g}$ , which translates to a minimum specific capacitance of 240 F/g (based on an average double layer capacitance of 20  $\mu\text{F}/\text{cm}^2$ ). The CV in Fig. 5A shows that the specific capacitance of a single activated carbon electrode is approximately 98 F/g. The lower capacitance arises due to the presence of a large number of micropores, which remain inaccessible to the electrolyte and hence do not lead to the formation of a double layer.<sup>1</sup> But better carbon materials have been synthesized. Firish reports 200 F/g for a carbon electrode with only 600  $\text{m}^2/\text{g}$  area.<sup>3</sup> Shi reports capacitance values upto 400 F/g for an activated carbon.<sup>1</sup>

Figure 5A also shows the CVs on the  $\text{RuO}_2$ -carbon composite in the same electrolyte. The CV curve exhibits ideal pseudocapacitive behavior between hydrogen and oxygen evolution reactions. The initial CV, as soon as the pellet is dipped in the electrolyte, shows less capacitance than the bare carbon itself. After electroless deposition the nanoparticles need to be converted to pseudocapacitive

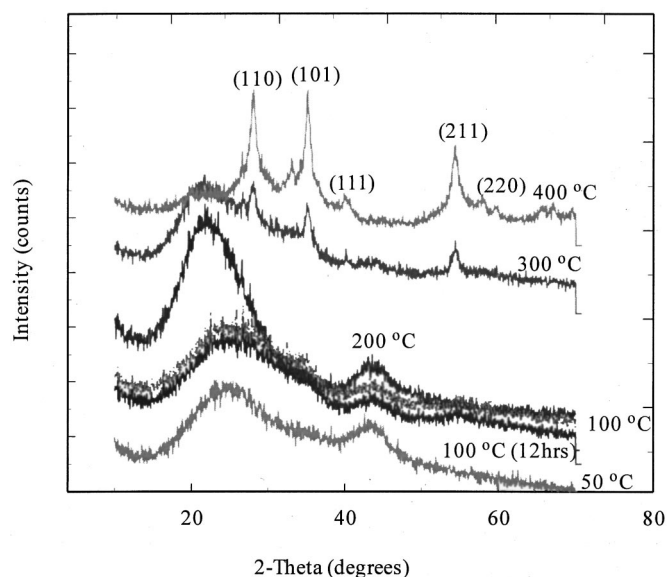


**Figure 3.** XRD patterns for Ru oxide-C composite annealed at different temperatures.

oxide-hydroxide form. This is achieved by electrochemical oxidation or by temperature treatment. The effect of heat-treatment on the specific capacitance is more pronounced than that by electrochemical treatment.

Figure 5B presents the CVs of electrochemically oxidized Ru. The oxidation was done at a potential of 0.75 V for 0, 0.5, 1, and 3 h. Electrochemical oxidation results in an increase in the specific capacitance of the material. After 30 min of oxidation most of the material becomes electrochemically active and increasing the oxidation time does not alter the capacitance significantly. However, the charge-discharge efficiency (ratio of anodic to cathodic currents) increases from 83 to 93% on increasing the oxidation time from 30 min to 3 h. No change in the current-potential response is seen for oxidation times higher than 3 h. According to Zheng *et al.*<sup>7,10</sup> the electrochemical reaction of  $\text{RuO}_2 \cdot x\text{H}_2\text{O}$  is similar to that of  $\text{RuO}_2$ . Ruthenium oxide and  $\text{RuO}_2 \cdot x\text{H}_2\text{O}$  can be oxidized and reduced reversibly through electrochemical protonation.<sup>14,15</sup>

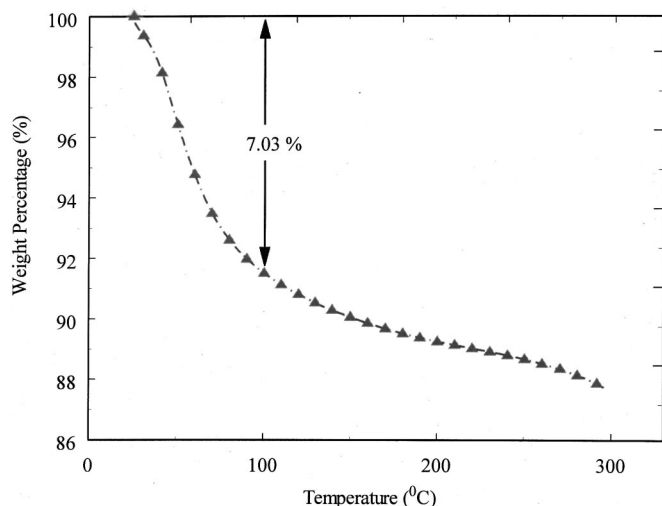
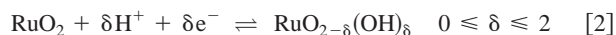
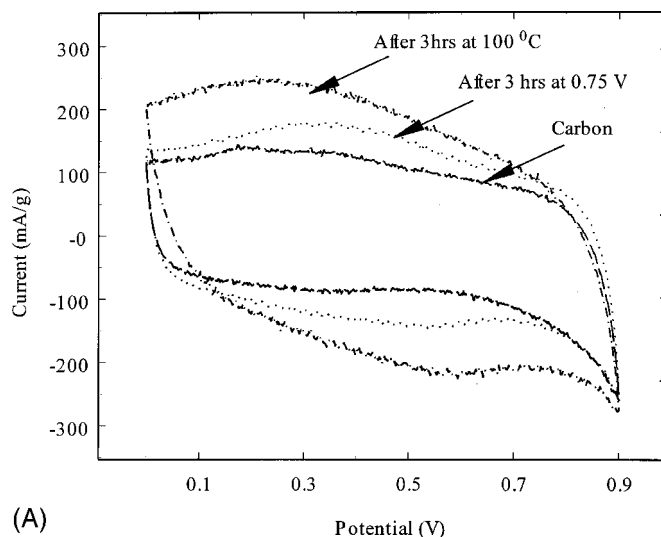
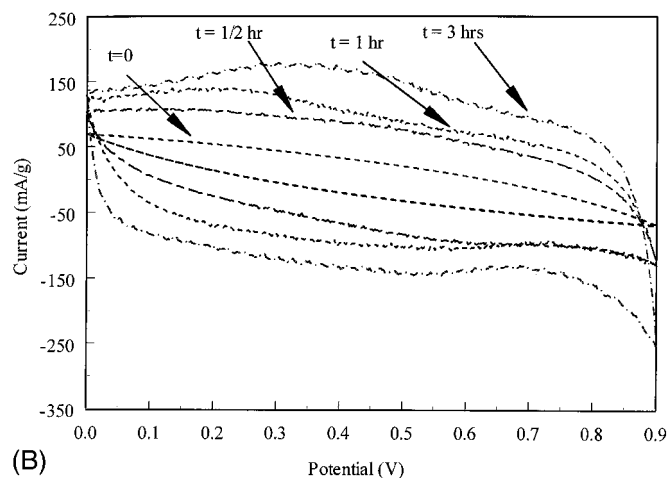


**Figure 4.** TGA analysis showing the weight loss of the Ru oxide composite with increase in temperature.



(A)



(B)

**Figure 5.** (A) Comparison of voltammograms of  $\text{RuO}_2\text{-C}$  treated at 100°C and after 3 h of electrochemical oxidation with bare carbon. (B) Comparison of CVs of a Ru oxide-C composite electrode after electrochemical oxidation for different times.

According to Hadzi-Jordanov *et al.*<sup>14</sup> oxidation of pure Ru in 1 N  $\text{H}_2\text{SO}_4$  results in the formation of an irreversible oxide. The formation of the irreversible oxide happens beyond 0.8 V vs. NHE (approximately 0.6 V vs. SCE). Upon repeated cycling to this potential, a new form of oxidized Ru is formed which exhibits complete reversibility<sup>14</sup> of the I-V profile. The Ru valency changed from 2 to 4 when the potential changed from 0 to 1 V, respectively. From Fig. 4b we get a specific capacitance of 140 F/g of total active material at a scan rate of 1 mV/s.

**Temperature treatment.**—The effect of temperature on the performance of the composites was investigated next. Figure 6 presents the CVs of the C- $\text{RuO}_2$  composite annealed at different temperatures. The composite was heated in an oxygen atmosphere for 3 h in all cases. As seen from Fig. 6, the specific capacitance increases with temperature and then starts decreasing. A maximum was observed at 100°C, where the specific capacitance is 190 F/g. At still higher temperatures, the capacitance drops significantly. At 200°C the capacitance was 170 F/g and on heating to 300°C the specific capacitance decreased to 120 F/g. At 400°C the capacitance dropped drastically to 87 F/g. The electrochemical oxidation of these electrodes was ineffective in improving the capacitance further.

A similar effect of temperature on the specific capacitance was also seen by Zheng *et al.*<sup>7,10</sup> They observed that the specific capaci-

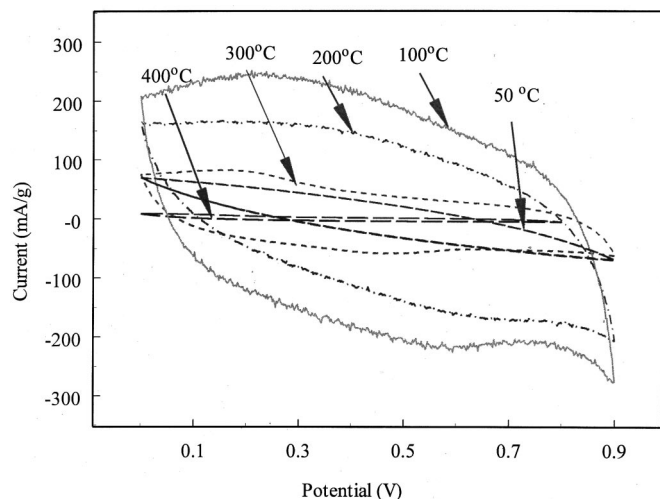
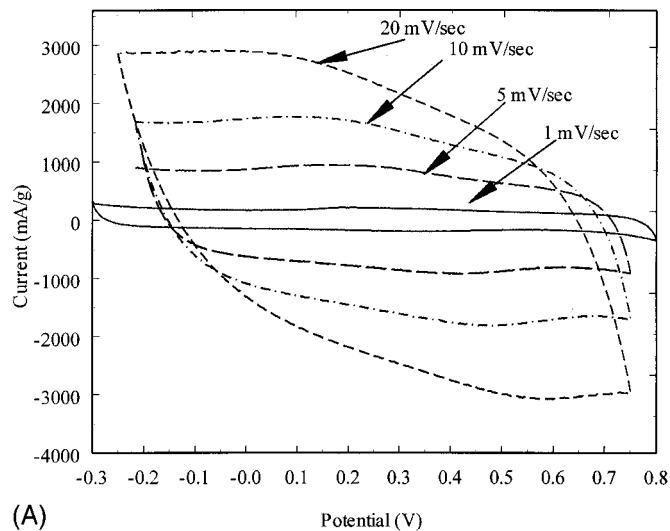


**Figure 6.** Comparison of CVs of pellets treated at different temperatures at 1 mV/s.

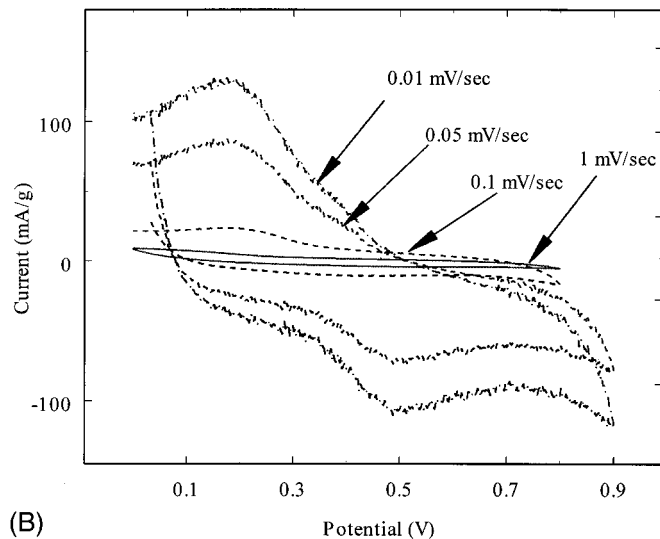
tance increases with heating, reaches a maximum and decreases rapidly beyond 150°C. Sol-gel derived hydrous ruthenium oxide, with two water molecules per  $\text{RuO}_2$  has a specific capacitance of 527 F/g. The specific capacitance reaches a maximum value of 720 F/g after annealing at 150°C.<sup>10</sup> According to McKeown *et al.*<sup>9</sup> charge storage in Ru oxide is maximized when the local structures retain facile transport pathways for both protons and electrons. This occurs when annealing the sample at 150°C leading to a final composition of  $\text{RuO}_2 \cdot 0.5\text{H}_2\text{O}$ . However, in our case the maximum capacitance occurs after heating the sample at 100°C. From the TGA (Fig. 4) we can see that the deposited sample loses 7 wt % water after heating to 100°C. At this stage the sample is  $\text{RuO}_2 \cdot 0.5\text{H}_2\text{O}$ , the composition at which maximum capacitance is realized. This is in agreement with the results reported by McKeown *et al.*<sup>9</sup> and Zheng *et al.*<sup>10</sup>

In both the sol-gel process and the electroless deposits, heating results in increasing the degree of crystallinity of the ruthenium. This decreases the rate of proton diffusion within the ruthenium. To investigate the effect of heating on the Ru oxide deposits, CVs were performed at different scan rates. Figure 7A presents the CVs for the 100°C annealed composite. The ratio of anodic to cathodic charge passed ( $Q_a/Q_c$ ) remains close to one in all cases. This indicates that the oxidation and reduction processes at the composite electrode interface are highly reversible. Further, the charge and discharge currents increase with scan rate, which is a characteristic feature of CVs. The influence of sweep rate on the performance of the composite electrode annealed at 400°C is shown in Fig. 7B. In this case, the charge and discharge currents decreased with increasing scan rate. This is exactly opposite of the behavior seen in Fig. 7A. Further, coulombic efficiency also reduced to 85% indicating some amount of irreversibility between the oxidation and reduction processes.

The reduced utilization of Ru could arise either from (i) decreased surface area or (ii) increased mass transfer limitations. The surface area of the composite heated at 400°C was determined by BET analysis. No change in the area was seen with heating (1080  $\text{m}^2/\text{g}$  at 400°C and 1060  $\text{m}^2/\text{g}$  at 100°C). Therefore, these results indicate that mass transfer limitations contribute to lowering the electrode specific capacitance at high oxidation temperatures. The proton diffusion rate is much slower in this case. On heating the composite, the degree of crystallinity increases and mass transport rates decrease. According to McKeown *et al.*,<sup>9</sup> the structure of  $\text{RuO}_x \cdot y\text{H}_2\text{O}$  materials correlates to their mixed conductivity and pseudocapacitance. As the degree of crystallinity increased the electronic conductivity increased while the proton transport rate decreased. Maximum capacitance was observed when both electron



(A)



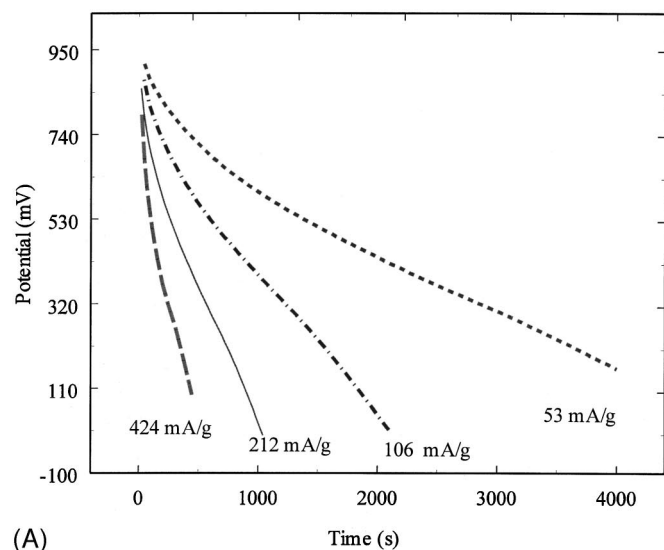
(B)

**Figure 7.** CVs of the composite electrode annealed at (A) 100°C and (B) 400°C at different scan rates.

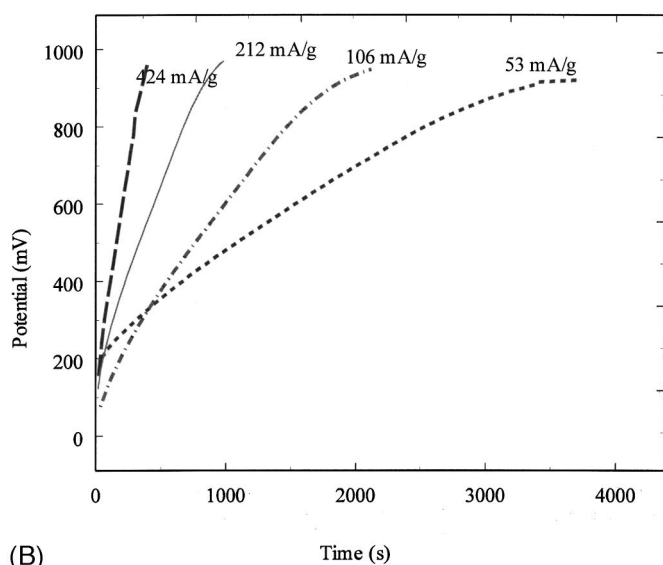
and proton transport were at an optimum. In our case, the optimum was seen at 100°C. In Fig. 7B, decreasing the scan rate allowed sufficient time for the proton to reach the surface of the oxide deposits and take part in the faradaic reaction given by Eq. 2. Hence, the currents in this case are much larger (100 mA/g at 0.01 mV/s) as compared to higher scan rates (20 mA/g at 1 mV/s). It is seen that the capacitance increases from 87 F/g at 0.1 mV/s to 140 F/g at 0.01 mV/s. The latter value at 0.01 mV/s is much closer to that of the material heated at 150°C. Reducing the scan rate more could yield a larger amount of the active material to be utilized, thereby increasing the capacitance further. This agrees with the results shown by McKeown *et al.*<sup>9</sup> Similar behavior (increased discharge currents at lower scan rates) has also been observed for metal hydride electrodes where the transport of hydrogen within the particle is rate limiting.<sup>16</sup>

**Charge-discharge studies.**—The capacitance obtained from CVs was confirmed by chronopotentiometric studies at various applied currents. Figure 8A presents the galvanostatic charge-discharge curves for the  $\text{RuO}_2$ -carbon composite heated at 100°C. The electrode was discharged from 0.9 to 0.1 V (Fig. 8A) at different specific currents. This results in reducing the valence state of Ru oxide from 4 to 2. The electrode was subsequently charged (oxidized) at





(A)



(B)

**Figure 8.** Chronopotentiograms for the pellet treated at 100°C at different currents, (A) discharge and (B) charge curves.

the same current (Fig. 8B). The times for both discharge and charge processes are very close to each other. This supports the fact that a redox transition between various oxidation stages in the Ru surface film is completely reversible. The high discharge rate studies confirm that the proton transport rate is very fast in the composite electrode. The specific capacitance ( $C$ ) was determined from the chronopotentiograms in Fig. 6 using<sup>17</sup>

$$C = \frac{ix\Delta t}{\Delta V} \quad [3]$$

where  $i$  is the specific discharge current applied for a time  $\Delta t$  to cause a potential change  $\Delta V$ . This also yields a specific capacitance of 190 F/g in agreement with the value obtained from the voltammograms. Figure 9 summarizes the capacitance values obtained from the charge-discharge studies for different composite annealing temperatures. The total capacitance for the composite increases from 98 F/g and a maximum of 190 F/g was observed at 100°C. Further increase in temperature results in decreasing the overall capacitance. The right y-axis shows the capacitance normalized to the Ru oxide content in the deposit. This was calculated after deducting the contribution due to the carbon substrate to the overall capacitance.

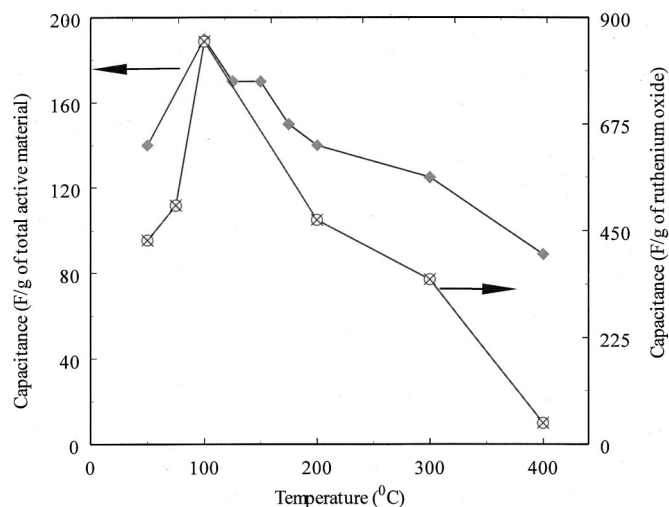


**Figure 9.** Change in capacitance of Ru oxide-C composites with temperature.

These results agree with the voltammograms shown in Fig. 6. The increase in capacitance for a hydrous  $\text{RuO}_2$ -carbon electrode as compared to bare carbon is shown clearly in Fig. 5A. For the same scan rate of 1 mV/s, a significant increase in the current is seen after loading Ru onto carbon. Further, since a small amount of Ru has been incorporated into carbon, this leads to better utilization of the Ru oxide as compared to bulk  $\text{RuO}_2$  particles.

In this study the amount of Ru deposited (9 wt %) was insufficient to cover the entire carbon substrate. Ru has been incorporated on carbon leading to the formation of thin clusters of Ru active sites. This can be seen from the TEM and EPMA pictures in Fig. 1b and 2, respectively. The BET surface area of the bare carbon was 1200  $\text{m}^2/\text{g}$ . After loading this with 9 wt %  $\text{RuO}_2$ , the BET surface area decreased to 1060  $\text{m}^2/\text{g}$ .  $\text{RuO}_2$  has a much higher bulk density (6.97  $\text{g}/\text{cm}^3$ ) as compared to activated carbon (0.2  $\text{g}/\text{cm}^3$ ). On loading  $\text{RuO}_2$  on carbon, the total weight of the composite increased for a given volume of material, due to the higher density of  $\text{RuO}_2$ . This resulted in reduction of the BET surface area, as this was normalized to the weight of the material. However, the volumetric surface area

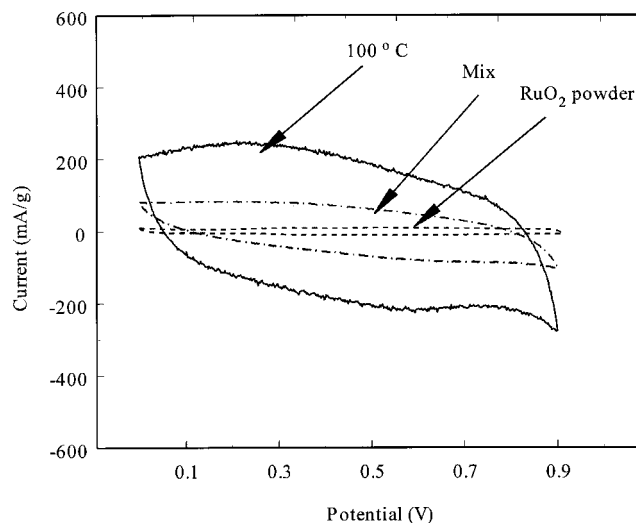


**Figure 10.** Comparison of CVs of Ru oxide-C composite pellet treated at 100°C with anhydrous  $\text{RuO}_2$  powder. CV of a mixture of anhydrous  $\text{RuO}_2$  (9 wt %) and carbon is also shown.

of the RuO<sub>2</sub>-C composite did not change significantly with increased ruthenium loading (214 m<sup>2</sup>/cm<sup>3</sup> for bare carbon to 207 m<sup>2</sup>/cm<sup>3</sup> for carbon with 9 wt % RuO<sub>x</sub>). Hence, the higher Ru utilization observed can be ascribed to the large surface area of carbon.

Figure 10 shows the comparison of CVs of RuO<sub>2</sub>-carbon treated at 100°C and pure RuO<sub>2</sub> powder. Results from a pellet electrode prepared by mixing the same percentage of ruthenium oxide powder (particle size <2 μm) with activated carbon as in the composite is also shown for comparison. The results clearly prove that the composite has a much higher specific capacitance as compared to crystalline RuO<sub>2</sub>. The superior performance of the composite electrode is due to utilization of the entire bulk of the RuO<sub>2</sub> nanoparticles on the surface of carbon.

### Conclusions

It has been demonstrated that hydrous metal oxide-carbon supercapacitors can be synthesized using an electroless deposition process. In this study activated carbon was loaded with 9 wt % Ru oxide. The effect of electrochemical oxidation and temperature treatment on the oxide was studied. It was shown that both methods increase the specific capacitance of the composites significantly. Ru valency changes from 2 to 4 on complete oxidation with proton diffusion within the bulk being the rate-determining step for the faradaic reaction. Increasing the time of electrochemical oxidation does not alter the capacitance significantly. However, increasing the oxidation temperature alters the capacitance drastically. The as-plated material exists in an amorphous form. Heating it increases the degree of crystallinity, which alters the proton diffusion rate within the film. This is reflected in the steep drop in capacitance on heating. A maximum capacitance of 190 F/g is observed after heating at 100°C. Miller *et al.*<sup>11</sup> report that a loading of 30 wt % Ru increases the specific capacitance of carbon from 95 to 190 F/g. Hence, electroless deposition leads to better utilization of the Ru deposited on carbon as compared to sputtering. Also, sputtering is expensive and cannot be applied on a large scale. The amorphous nature of the electroless deposits offers an opportunity to synthesize composite RuO<sub>2</sub>-carbon composites, which possess much larger energy and

power densities compared to that of bare carbon. Further development work is needed before these materials can be used in supercapacitor devices. Specifically, the high discharge-rate characteristics of these materials need to be improved further by preparing thinner electrodes with lower ohmic resistance.

### Acknowledgments

Financial support by the Department of Energy under the DOE-EPSCOR program is acknowledged gratefully.

*The University of South Carolina assisted in meeting the publication costs of this article.*

### References

1. H. Shi, *Electrochim. Acta*, **41**, 1633 (1996).
2. B. E. Conway, *Electrochemical Supercapacitors, Scientific Fundamentals and Technological Applications*, Kluwer Academic/Plenum Publications, New York (1999).
3. D. W. Firsich, in *Electrochemical Capacitors II*, F. M. Delnick, D. Ingersoll, X. Andrieu, and K. Naoi, Editors, PV 96-25, p. 235, The Electrochemical Society Proceedings Series, Pennington, NJ (1997).
4. V. Srinivasan and J. W. Weidner, *J. Electrochem. Soc.*, **144**, L210 (1997).
5. K.-C. Liu and M. A. Anderson, *J. Electrochem. Soc.*, **143**, 124 (1996).
6. I. D. Raistrick, in *Electrochemistry of Semiconductors and Electrodes*, J. McHardy and F. Ludwig, Editors, p. 297, Noyes Publications, Park Ridge, NJ (1992).
7. J. P. Zheng and T. R. Jow, *J. Electrochem. Soc.*, **142**, L6 (1995).
8. C. Lin, J. A. Ritter, and B. N. Popov, *J. Electrochem. Soc.*, **146**, 3155 (1999).
9. D. A. McKeown, P. L. Hagans, L. P. L. Carette, A. E. Russel, K. E. Swider, and D. R. Rolison, *J. Phys. Chem. B*, **103**, 4825 (1999).
10. J. P. Zheng, P. J. Cygan, and T. R. Jow, *J. Electrochem. Soc.*, **142**, 2699 (1995).
11. J. M. Miller, B. Dunn, T. D. Tran, and R. W. Pekala, *J. Electrochem. Soc.*, **144**, L309 (1997).
12. J. M. Miller and B. Dunn, *Langmuir*, **15**, 799 (1999).
13. G. G. Gawrilov, *Chemical Nickel Plating*, Portcullis Press Ltd., Surrey, England (1979).
14. S. Hadzi-Jordanov, H. Angerstein-Kozłowska, M. Vukovic, and B. E. Conway, *J. Electrochem. Soc.*, **125**, 1471 (1978).
15. B. E. Conway, in *New Sealed Rechargeable Batteries and Supercapacitors*, B. M. Barnett, E. D'Agostino, G. Halpert, Y. Matsuda, and Z.-i. Takehara, Editors, PV 93-23, p. 15, The Electrochemical Society Proceedings Series, Pennington, NJ (1993).
16. B. S. Haran, B. N. Popov, and R. E. White, *J. Electrochem. Soc.*, **145**, 3000 (1998).
17. A. W. Goldenstein, W. Rostoker, W. Schossberger, and G. Gutzeit, *J. Electrochem. Soc.*, **104**, 104 (1957).